Climate overshoot and the insurability frontier: peak stress, domestic capacity, and market retreat risk*

*Architesh Panda, architesh.panda@sei.org, Stockholm Environment Institute (SEI), Bangkok, Thailand

Keywords: *climate overshoot; insurability; climate finance; insurance market exit; SSP5-3.4-OS;*

Author Statement:

This is a non-peer reviewed version/pre-print of the paper.

Architesh Panda, 2026

Abstract

Climate overshoot can create mid-century peaks in climate stress before end-century temperatures stabilize, but its implications for insurance availability remain poorly understood. We assess subnational insurance market exit risk under overshoot across 1,590 first-order administrative regions in 88 countries, covering 4.54 billion people. Combining ADM1-level multi-hazard climate stress, an eight-model SSP5-3.4-OS overshoot signal and a country-level domestic capacity index, we identify where overshoot-adjusted risk pressure approaches an insurability boundary. Relative to baseline climate stress, overshoot increases risk pressure in 75.9% of regions and exposes an additional 59 million people to high uninsurability risk. Six regions, five in Sudan and one in Bangladesh, meet the strict boundary-zone condition of extreme risk pressure and very low capacity. A wider near-boundary frontier contains 87 regions and 561 million people, while a capacity threshold near 0.40 separates buffered from vulnerable systems. These results show that overshoot affects insurance-relevant risk through the timing of peak stress, making pre-emptive climate financing and capacity-building central to preserving insurability and limiting wider climate-financial instability.

Introduction

Insurability, the degree to which insurance coverage remains available and affordable, is already under pressure from more frequent and severe climate-related hazards. Rising losses are translating into higher premiums, tighter underwriting and insurer withdrawal in exposed regions, just as financial protection becomes most needed in many low- and middle-income countries [1,2]. These pressures may become harder to manage under climate overshoot: the growing possibility that the Paris Agreement's 1.5 °C target will be temporarily exceeded before temperatures later decline through net-negative CO_2 emissions [4,5].

Recent experience in California's wildfire and Florida's hurricane exposed property market shows that restoring insurance coverage in stressed markets depends on regulatory redesign and renewed underwriting capacity, not simply on changes in hazard conditions or risk reduction [8–10]. Under climate overshoot, this creates a critical timing problem. Even if temperatures later moderate, temporary mid-century risk spikes may induce market exits that persist beyond the period of peak hazard, pushing places across insurability thresholds during a stress window when recovery may prove institutionally difficult. For insurers, that timing matters because pricing, underwriting and capital allocation respond to conditions during the period of peak stress, not to eventual climatic recovery [8,11,12].

The implications are different in low-income countries, where insurance penetration, domestic underwriting capacity and public fiscal buffers are already limited [48]. In these settings, overshoot may not only trigger withdrawal from existing markets; it may also prevent risk-transfer systems from scaling before climate stress peaks [49,50]. This matters because disaster finance in many vulnerable countries remains largely ex post rather than pre-arranged, leaving governments and households exposed when shocks occur [49]. At the same time, adaptation finance flows to developing countries remain far below estimated needs, limiting investment in the risk reduction, data infrastructure and institutional capacity needed to make insurance viable [51]. For low-capacity countries, the insurability question is therefore also a climate-finance question: whether public balance sheets, sovereign risk pools, premium support and local risk information can be strengthened before the mid-century overshoot window arrives [17,18,25,26].

Once insurers retreat from a market, re-entry may remain difficult even if physical hazards later moderate, particularly where renewed underwriting depends on regulatory reform, reinsurance support or other forms of financial innovation. Insurance retreat therefore matters not only as a financial outcome, but as an early warning that climate risk is approaching the limits of commercially viable risk transfer. Where coverage becomes unaffordable or unavailable, effects can propagate into housing markets, lending, post-disaster reconstruction and public budgets [1,2,22–25].

Prior work has examined insurability through the lenses of risk-based pricing, disaster finance and market design, revealing tensions between efficiency, equity and the limits of private risk transfer under intensifying climate stress. One strand shows that risk-based pricing can improve efficiency and encourage household adaptation, but that these gains require complementary public investments for example in flood protection and large-scale risk reduction [13–15]. A parallel literature argues that governing adaptation through private insurance can individualize responsibility for systemic climate harms and produce inequitable outcomes when pricing renders coverage unaffordable [16]. More recent work suggests that where private coverage fails, public backstops and hybrid arrangements are most durable when embedded within broader risk-reduction strategies rather than treated as substitutes for adaptation [3,17–19].

Yet this literature has not addressed climate overshoot. Overshoot is not simply a higher level of warming; it introduces a bounded mid-century period in which risk intensifies precisely when investment, underwriting and adaptation decisions for long-lived assets are most consequential [5–7]. Existing work on insurance crises and market volatility has largely focused on contemporary hazards, present-day pricing stress and near-term policy responses [3]. It has not asked how overshoot might alter the timing and geography of insurability itself, or whether regions may cross an insurability threshold during the overshoot window that proves difficult to reverse thereafter. Understanding where and when overshoot approaches insurability boundaries is therefore essential for targeting adaptation finance, designing risk-transfer instruments and preventing protection-gap-driven inequality. Further, Subnational resolution is equally essential. A country may appear broadly insurable while containing regions already close to a threshold of market failure [20].

This study addresses those gaps by developing, to our knowledge, the first global subnational assessment of insurance market exit risk under climate overshoot. The analysis covers 1,590 first-level administrative regions across 88 countries and 4.54 billion people, integrating multi-scenario CMIP6 climate projections with a composite domestic capacity index that captures the institutional and financial conditions needed to absorb rising insurance stress. It introduces an overshoot adjustment to account for non-monotonic warming trajectories and identifies where high climate stress and low domestic capacity combine to push regions toward an insurability boundary. The results show that overshoot sharpens an insurability boundary rather than intensifying risk uniformly, with the greatest pressures concentrated in low-capacity regions, a critical capacity threshold near 0.40 and a distinct capacity-erosion dynamic in higher-capacity markets.

Data and Methods

Study domain and spatial unit

The analysis is conducted at the level of first-order administrative regions (ADM1). The spatial backbone is derived from GADM 4.1, which provides global subnational boundary polygons [28]. The final analytical sample includes 1,590 ADM1 regions across 88 countries, covering approximately 4.54 billion people. Climate processing and intermediate overlays were first conducted on a broader ADM1 universe, after which the

manuscript sample was restricted to countries with complete information for all six domestic-capacity components.

The complete-case rule was applied because the framework combines subnational climate risk with country-level institutional and financial capacity. Retaining countries with missing values in any capacity component would have produced inconsistent measurement across the sample. Sensitivity checks using relaxed capacity rules are therefore treated as supplementary rather than as the headline specification. Country-level domestic capacity values are assigned to all ADM1 regions within each country. This is a limitation, since within-country variation in insurance access, fiscal support, regulatory capacity and local market withdrawal is not directly observed.

Climate stress index

Climate risk pressure is measured using a multi-hazard stress index at ADM1 resolution. The index combines three hazard streams: temperature and precipitation change from CMIP6 projections, extreme precipitation, and observed fire-weather exposure. CMIP6 projections follow the CMIP6 experimental design and ScenarioMIP protocol [29,30]. The primary tier uses MIROC6 large ensembles, with 50 members for SSP2-4.5 and SSP5-8.5 and 10 members for SSP1-2.6 and SSP3-7.0 [31]. A cross-model tier uses eight CMIP6 models: MIROC6, CanESM5, GFDL-ESM4, IPSL-CM6A-LR, MRI-ESM2-0, BCC-CSM2-MR, MPI-ESM1-2-LR and INM-CM5-0 [31–38].

For each ADM1 region, multi-model medians and interquartile ranges are calculated for daily maximum temperature, mean temperature and precipitation, comparing a 2021–2040 baseline with a 2081–2100 end-century window. Extreme precipitation is represented by RX5-day, the annual maximum consecutive five-day precipitation total, computed from daily precipitation and aggregated to ADM1 zonal means [39]. Fire-weather exposure is represented by the Canadian Fire Weather Index, using Copernicus/ECMWF fire-weather products and the 2001–2020 mean annual maximum Fire Weather Index [40–42].

The final climate stress index is a percentile-ranked composite of multi-model median daily maximum temperature, RX5-day extreme precipitation and observed Fire Weather Index climatology. Each component is standardized independently across the ADM1 sample before aggregation. The resulting index ranges from 0 to 1, with higher values indicating greater multi-hazard climate stress. The index is therefore a relative global measure of multi-hazard pressure rather than a direct estimate of insured loss.

Overshoot adjustment

Standard end-century metrics can understate insurance stress under overshoot because they do not capture the mid-century period when warming peaks before later partial recovery. SSP5-3.4-OS was designed within ScenarioMIP to examine a substantial twenty-first-century overshoot pathway [30]. For each model and ADM1 region, daily maximum temperature is extracted for the 2021–2040 baseline, the mid-century peak decade and the 2091–2100 recovery window. The overshoot spike is defined as the difference between mid-century peak temperature and end-century temperature.

For each ADM1 region, overshoot probability, π, is calculated as the fraction of the eight-model ensemble showing a positive overshoot spike. The overshoot signal is embedded through a convex combination:

$$R_{pen} = (1 - \omega)R_{robust} + \omega\pi$$

where R_{robust} is the baseline risk-pressure index and ω is the overshoot embedding weight. The headline specification uses $\omega = 0.15$. Because this is a convex combination, R_{pen} can be higher or lower than R_{robust}, depending on whether the overshoot signal exceeds baseline stress. The adjustment is intentional: it does not assume that overshoot directly causes market exit risk, but treats overshoot as an additional timing-sensitive signal in the risk-pressure index.

Domestic capacity index

Domestic absorptive capacity, C, is represented by a country-level composite index capturing institutional, fiscal and insurance-market conditions. The index combines six components: non-life insurance premiums as a percentage of GDP, insurance sector assets as a percentage of GDP, government revenue excluding grants, government debt, ND-GAIN readiness and ND-GAIN vulnerability [43–47]. Government debt and ND-GAIN vulnerability are inverted so that higher values consistently indicate greater capacity.

The weights are 0.20 for non-life insurance premiums, 0.15 for insurance sector assets, 0.15 for government revenue, 0.10 for government debt, 0.15 for ND-GAIN readiness and 0.25 for inverted ND-GAIN vulnerability. All components are converted to percentile ranks before aggregation, and extreme values are winsorized at the 1st and 99th percentiles. The resulting capacity index ranges from 0 to 1; in the corrected sample, it ranges from 0.073 to 0.853.

Uninsurability index and regime classification

The uninsurability index combines overshoot-adjusted climate risk pressure with domestic capacity deficit:

$$UI_{robust} = 0.6R_{robust} + 0.4(1 - C)$$
$$UI_{pen} = 0.6R_{pen} + 0.4(1 - C)$$

The headline results use UI_{pen}. The index is used as a continuous ranking metric rather than as the sole basis for categorical regime assignment.

Each ADM1 region is classified into one of four regimes using the interaction between R_{pen} and C. Stable insurability refers to regions where climate stress remains compatible with market functioning under prevailing capacity. Underinsurance refers to regions where limited capacity constrains protection despite non-extreme stress. Strained insurability captures elevated stress with constrained capacity. Boundary-zone regions represent potential market-exit risk and are defined by the strict joint condition $R_{pen} > 0.90$ and $C < 0.20$. A near-boundary frontier is defined using UI_{pen} values between 0.75 and 0.85.

The boundary-zone rule is intentionally stricter than the uninsurability index alone. A region must jointly satisfy extreme risk pressure and very low capacity to be classified as boundary zone. This avoids treating high-hazard but high-capacity regions as immediate market-exit cases, while still allowing them to appear in the near-boundary or capacity-erosion discussion.

Sensitivity analysis

Sensitivity checks vary ω from 0 to 0.30 and recalculate R_{pen}, UI_{pen} and regime assignments at each value. Additional checks evaluate supplementary hazard-layer integrations, including RX5-day extreme precipitation outputs and fire-weather-enriched files. Across these checks, the central qualitative result is stable: overshoot increases insurance-relevant risk pressure for most regions, the sharpest boundary risks remain concentrated in low-capacity settings and a broader near-boundary frontier extends beyond the six strict boundary-zone cases.

Results

Global insurability regimes under climate overshoot

Using the overshoot-adjusted risk-pressure index and domestic capacity measure described above, we classify each ADM1 region into four regimes: stable insurability, underinsurance, strained insurability and boundary zone. Across 1,590 regions in 88 countries, most regions remain stable, but severe stress is concentrated in a smaller set of low-capacity regions (Table 1; Fig. 1).

Stable insurability accounts for 1,464 regions, or 92.1% of the sample, covering 4,077.9 million people. A further 83 regions are classified as underinsurance, 37 as strained insurability and 6 as boundary zone. In population terms, 465.4 million people already live outside the stable regime. This distribution shows that overshoot does not generate uniform global deterioration; it sharpens an uneven frontier where climate pressure and weak absorptive capacity intersect.

The 465.4 million people outside stable insurability are not distributed evenly across regimes. Most are in the underinsurance regime: 83 regions containing 275.8 million people where climate pressure is not yet extreme, but institutional and financial capacity is too weak to sustain effective protection. A further 37 regions, containing 167.3 million people, are already strained, where elevated climate stress and limited capacity increasingly converge. The six boundary-zone regions, containing 22.2 million people, represent the acute edge of this process rather than its full extent.

The regime structure also shows why hazard alone is insufficient. Many high-stress regions remain stable because domestic capacity buffers the shock, while some lower-stress regions enter underinsurance because institutional and fiscal capacity is too weak. The boundary zone should therefore be read not as an exhaustive count of uninsurability, but as the acute edge of a broader process. The small number of boundary-zone cases identifies only the most acute combinations of extreme risk pressure and very low capacity. Its analytical value lies in marking the frontier of breakdown under overshoot, while a much larger group sits close to that frontier. Much of the policy-relevant action occurs before a region crosses the strict boundary. Underinsurance and strained insurability describe intermediate states in which markets may still exist but are increasingly incomplete, unaffordable or dependent on public support. These transitional regimes are central to adaptation planning because they mark where targeted investment can still prevent a shift from coverage stress to coverage retreat.

Boundary zones and the near-boundary frontier

Six regions meet the strict boundary-zone condition, defined as overshoot-adjusted risk pressure above 0.90 and domestic capacity below 0.20 (Table 2; Fig. 1b). Five are in Sudan — North Darfur, East Darfur, West Darfur, Kassala and River Nile — and one is in Bangladesh, Mymensingh. Together they contain 22.2 million people. Their common feature is not hazard intensity alone, but the combination of extreme climate stress with exceptionally weak institutional and financial capacity.

Sudan's boundary-zone regions share the lowest capacity value in the sample and combine very high fire-weather exposure with extreme risk-pressure values. Bangladesh's Mymensingh is structurally different: its capacity is higher than Sudan's, but the region contains a much larger exposed population and faces compound stress from heat, monsoon variability and cyclone-related risk. The two cases therefore illustrate different routes into the same boundary-zone classification.

A wider near-boundary frontier contains 87 regions and approximately 561 million people, defined by uninsurability index values between 0.75 and 0.85 (Extended Data Table 1). These regions include parts of

Ethiopia, Bangladesh, Nepal, India, Bolivia, Zambia, Cameroon and Mongolia. Several remain formally stable only because capacity buffers very high risk pressure. Examples include Karnali and Sudurpaschim in Nepal, Ladakh in India, Cochabamba in Bolivia and Ulaanbaatar in Mongolia. These are not securely stable regions; they are buffered regions whose classification depends on continued institutional and financial support.

The most important near-boundary cases are not necessarily those with the lowest capacity. Several regions remain formally stable despite very high risk pressure because national capacity still buffers local exposure. Their stability is therefore conditional: it depends on fiscal space, regulatory effectiveness, reinsurance access and the continued willingness of public or private institutions to absorb rising losses. The near-boundary frontier should therefore be read as a list of buffered vulnerability, not as a list of regions already beyond repair. Boundary-zone regions already require external support because conventional market solutions are unlikely to remain sufficient. Near-boundary regions still offer scope for preventive action through adaptation finance, public reinsurance, risk reduction and capacity-building before full market-exit risk emerges.

Taken together, the six boundary-zone regions and the broader near-boundary frontier show that overshoot sharpens insurability stress along a steep gradient rather than producing smooth global deterioration. The geography of emerging uninsurability is layered: a small number of acute exit-risk regions sit at the leading edge, but they are surrounded by a much larger set of regions that could cross the boundary under plausible future climate stress or modest capacity erosion.

Overshoot adjustment and regime shifts

The overshoot adjustment captures a clear temporal asymmetry under SSP5-3.4-OS. Across 3,222 ADM1 regions with valid projections in the eight-model ensemble, 3,092 regions (95.9%) show a positive ensemble-median overshoot spike, meaning that mid-century peak temperature exceeds end-century temperature after partial recovery. The mean spike is 0.313 °C and the maximum is 1.025 °C (Fig. 2). This temporal structure matters because insurance markets respond to the period when stress is highest, not to the eventual end state. Under SSP5-3.4-OS, end-century temperatures may moderate after the deployment of carbon dioxide removal, but the mid-century peak still creates a stress window during which underwriting, pricing and capital-allocation decisions are made. In that sense, overshoot changes not only the level of climate risk, but its decision-relevant timing.

Embedding this signal into the risk-pressure index changes insurability patterns in a systematic but non-uniform way. At the headline embedding weight of omega = 0.15, overshoot-adjusted risk pressure exceeds the robust baseline in 1,207 of 1,590 regions (75.9%), with a mean uplift of Delta R = +0.038. The increase is concentrated most visibly in the high-pressure, low-capacity quadrant of the risk-pressure and capacity space (Fig. 3). Because the adjusted index is a convex combination of baseline stress and overshoot spike probability, it can either increase or decrease relative to baseline stress. This produces negative Delta R in 383 regions, where persistent baseline stress is greater than the overshoot spike signal. The regime consequences are limited but meaningful: 26 regions change regime after the overshoot adjustment, indicating that the classification is broadly stable even as risk pressure shifts across most of the sample.

The sensitivity analysis supports this interpretation. As omega increases from zero to 0.30, the mean uplift in risk pressure rises approximately linearly, but the share of regions with positive Delta R remains fixed at 75.9% for all omega values above 0.05. This means the geography of worsening is determined mainly by the relationship between baseline stress and overshoot probability, while the weight controls the magnitude of the adjustment. The limited number of regime shifts is itself informative: the classification is not being driven mechanically by the overshoot adjustment, while the continuous risk-pressure metric still captures widespread

deterioration within regimes. In practical terms, overshoot changes the intensity and timing of stress more than it redraws the entire global map. This strengthens the interpretation of the boundary zone as a conservative leading edge, with broader deterioration occurring across the surrounding frontier.

High-income erosion and hazard contrasts

High-income countries face a different insurability challenge. None enters the strict boundary zone because domestic capacity remains high, but this stability is conditional. The United States records a mean overshoot-adjusted risk pressure of 0.758 across 56 ADM1 regions. It remains stable because national capacity is high, yet insurer retreat, residual-market dependence and catastrophe-model reform in California's wildfire-exposed property market and Florida's hurricane-exposed property market show that effective local capacity is already eroding in some states [1,8,9,11].

Within the United States, the highest risk-pressure values are not confined to the iconic wildfire states. Several central and eastern states show high composite risk pressure, reflecting heat-humidity compounding, agricultural drought and flooding. Western states remain critical because they combine very high fire-weather exposure with visible insurer withdrawal. This creates a mismatch between national capacity, which appears high, and local effective capacity, which may already be substantially lower in stressed insurance markets. Australia shows a related but more hazard-specific pattern. It has the highest mean wildfire stress among high-income countries in the sample, with several states exposed to both high current fire weather and large overshoot spikes. National capacity continues to buffer these exposures, but rapid premium increases in bushfire corridors suggest that this buffer is under pressure.

These high-income cases should be interpreted as capacity-erosion cases, not as evidence of current boundary-zone failure. Market exit has not generalized because domestic capacity, public backstops and financial depth still absorb rising losses. But the adjustment burden is already visible through non-renewal, premium escalation and increased reliance on residual mechanisms. High-income countries are therefore not outside the insurability problem; they occupy an earlier phase of it.

Hazard contrasts reinforce the point. Cyclone exposed regions show a mean increase in uninsurability 1.7 times larger than wildfire-exposed regions. Mean Delta UI is +0.033 in cyclone zones compared with +0.020 in wildfire zones, and 80% of cyclone-exposed regions worsen under the overshoot-adjusted framework compared with 59% of wildfire-exposed regions (Fig. 4). This divergence suggests that the most severe overshoot-related deterioration is concentrated in tropical cyclone regions where physical exposure combines with weaker fiscal, regulatory and insurance capacity [27].

This hazard contrast also helps rebalance the empirical narrative away from the cases that dominate public debate. Wildfire-related insurance withdrawal in California and Australia is visible because these are high-value, well-documented markets. The larger overshoot-related deterioration, however, is concentrated in tropical cyclone settings where exposure intersects with thinner fiscal buffers, lower insurance penetration and greater dependence on international reinsurance. The result is not that wildfire markets are safe, but that cyclone-exposed developing regions face a steeper path from rising hazard to protection failure [27].

Discussion and conclusion

The results show that climate overshoot does not raise insurability risk uniformly. Instead, it sharpens a boundary crossed first where extreme climate stress converges with weak domestic capacity. The six boundary-zone regions mark the leading edge of market-exit risk, while the 87-region near-boundary frontier shows where preventive intervention remains plausible. The main policy story is therefore not generalized global uninsurability, but a steep and uneven frontier of climate-financial vulnerability.

Overshoot matters because it changes the timing of insurance relevant risk. Across the overshoot ensemble, 95.9% of regions show a positive spike, and embedding this signal increases risk pressure in 75.9% of regions. Insurance markets respond to peak-stress conditions, not eventual temperature recovery. Overshoot therefore creates a bounded window during which withdrawal decisions, reinsurance repricing and public backstop expansion may become institutionally entrenched. This is consistent with overshoot-equity scholarship, which argues that responsibilities persist through obligations for support, drawdown and repair [5–7,21]. The findings also show that insurability is co-produced by physical hazard and domestic capacity. Regions with very high risk pressure do not necessarily enter the boundary zone if institutional and financial capacity remain strong, while others approach it at lower hazard levels because capacity is weak. The capacity threshold near 0.40 suggests that protection-gap dynamics should be treated as climate-financial vulnerability rather than as hazard exposure alone [17,26].

This helps reconcile low-capacity boundary cases with high-income erosion cases. Sudan and Bangladesh appear at the acute edge because weak capacity coincides with high stress. The United States and Australia remain outside the boundary zone because aggregate capacity is high, yet they already show insurer retreat, premium escalation and residual-market dependence. Emerging uninsurability is therefore sequential rather than binary: low-capacity regions cross thresholds first, while high-capacity markets experience slower erosion. The consequences extend beyond insurance. Where coverage becomes unaffordable or unavailable, effects can propagate into mortgages, credit, business continuity, property values and public budgets [22–25]. Insurability should therefore be treated as an early-warning indicator of climate-financial instability, not merely as a private-sector affordability problem.

Two policy implications follow. First, insurance cannot be treated as a stand-alone adaptation solution; risk transfer will remain durable only when combined with risk reduction, public backstops and institutional strengthening. Second, the policy frontier extends beyond the six strict boundary-zone cases. The near-boundary analysis identifies where targeted adaptation finance, public support for risk reduction and carefully designed insurance mechanisms may still prevent market-exit risk. In an overshoot world, this also raises distributive questions because the regions least able to absorb market retreat are often not those most responsible for overshoot.

Waiting for observed market exit would mean acting after the peak-stress window has already forced repricing, non-renewal or reliance on residual public mechanisms. Earlier intervention should focus on improving local risk information, strengthening public finance, supporting risk pools and linking premium support to measurable risk reduction. Adaptation finance is therefore not only a recovery tool but a pre-emptive way to preserve insurability before markets retreat. This study has limitations. It does not model insurer behaviour or firm-level withdrawal decisions, and the domestic capacity index is a country-level proxy for a more complex institutional reality. The framework identifies exposure to market-exit risk, not literal predictions of withdrawal. The thresholds are operational and should be calibrated further against observed market exits, including California, Florida and other stressed markets. These caveats do not alter the central conclusion: under climate overshoot, insurability becomes a boundary problem shaped by timing and capacity, not merely by end-century hazard severity.

Data availability

The processed ADM1-level analytical data and supplementary tables will be made available in a public repository before publication.

Code availability

The processed ADM1 analytical dataset and scripts required to reproduce all manuscript tables and figures are organized in a replication package and will be deposited in a public repository upon acceptance. The package reproduces the submitted results from processed data; raw CMIP6 and geospatial preprocessing steps are documented separately because they rely on large external archives.

Acknowledgements

No funding has been provided for this research.

Author contributions

A.P. conceived the study, designed the analytical framework, processed and analysed the data, prepared the figures and tables, and wrote the manuscript.

Competing interests

The author declares no competing interests.

Declaration of generative AI and AI-assisted technologies

Generative AI tools were used for some language editing. All analyses, data, results and final manuscript content were verified by the author.

References

1. Jones, D. The uninsurable future: the climate threat to property insurance, and how to stop it. Yale Law J. Forum 135, 181-236 (2025).

2. Jarzabkowski, P., Meissner, K. & Mason, M. Insurance options in a climate changed future: the way forward for urban climate policy and practice. J. City Clim. Policy Econ. https://doi.org/10.3138/jccpe-2024-0029 (2025).

3. Kousky, C., Treuer, G. & Mach, K. J. Insurance and climate risks: policy lessons from three bounding scenarios. Proc. Natl Acad. Sci. USA 121, e2317875121 (2024).

4. IPCC. Climate Change 2023: Synthesis Report. Contribution of Working Groups I, II and III to the Sixth Assessment Report of the Intergovernmental Panel on Climate Change (IPCC, 2023).

5. Schleussner, C.-F. et al. Overconfidence in climate overshoot. Nature 634, 366-373 (2024).

6. McLaren, D. P. & Markusson, N. The co-evolution of technological promises, modelling, policies and climate change targets. Nat. Clim. Change 10, 392-397 (2020).

7. Rogelj, J. et al. Scenarios towards limiting global mean temperature increase below 1.5 °C. Nat. Clim. Change 8, 325-332 (2018).

8. Congressional Budget Office. Climate Change, Disaster Risk, and Homeowner's Insurance (CBO, 2024).

9. California Department of Insurance. Reform Made Real: California Department of Insurance Completes Final Evaluation of Innovative Forward-Looking Model to Address California's Coverage Crisis (CDI, 2025).

10. Florida Office of Insurance Regulation. Commissioner Mike Yaworsky Approves Over 10 Property & Casualty Insurers to Enter the Market Following Historic Reforms (FLOIR, 2025).

11. National Association of Insurance Commissioners. NAIC Catastrophe Modeling Primer (NAIC, 2025).

12. American Academy of Actuaries. The Insurance Impact of Climate Change Catastrophes (American Academy of Actuaries, 2023).

13. de Ruig, L. T., Haer, T., de Moel, H., Botzen, W. J. W. & Aerts, J. C. J. H. How the USA can benefit from risk-based premiums combined with flood protection. Nat. Clim. Change 12, 995-1001 (2022).

14. Hudson, P., Botzen, W. J. W. & Aerts, J. C. J. H. Flood insurance arrangements in the European Union for future flood risk under climate and socioeconomic change. Glob. Environ. Change 58, 101966 (2019).

15. Surminski, S. & Thieken, A. H. Promoting flood risk reduction: the role of insurance in Germany and England. Earth's Future 5, 979-1001 (2017).

16. Lucas, C. H. & Booth, K. I. Privatizing climate adaptation: how insurance weakens solidaristic and collective disaster recovery. WIREs Clim. Change 11, e676 (2020).

17. Clarke, D. J. & Dercon, S. Dull Disasters? How Planning Ahead Will Make a Difference (Oxford Univ. Press, 2016).

18. Linnerooth-Bayer, J. & Hochrainer-Stigler, S. Financial instruments for disaster risk management and climate change adaptation. Clim. Change 133, 85-100 (2015).

19. Mechler, R. et al. Managing unnatural disaster risk from climate extremes. Nat. Clim. Change 4, 235-237 (2014).

20. Panda, A. Uninsurable Futures: Climate Risk and Emerging Protection Gaps in India (SSRN, doi.org/10.2139/ssrn.5568959, 2025).

21. Pelz, S. et al. Using net-zero carbon debt to track climate overshoot responsibility. Proc. Natl Acad. Sci. USA 122, e2409316122 (2025).

22. Network for Greening the Financial System. NGFS Climate Scenarios for Central Banks and Supervisors (NGFS, 2023).

23. Bernstein, A., Gustafson, M. T. & Lewis, R. Disaster on the horizon: the price effect of sea level rise. J. Financ. Econ. 134, 253-272 (2019).

24. Hino, M. & Burke, M. The effect of information about climate risk on property values. Proc. Natl Acad. Sci. USA 118, e2003374118 (2021).

25. WWF. Tackling the Insurance Protection Gap: Leveraging Climate Mitigation and Nature to Increase Resilience (WWF, 2025).

26. Carter, M. R., de Janvry, A., Sadoulet, E. & Sarris, A. Index insurance for developing country agriculture: a reassessment. Annu. Rev. Resour. Econ. 9, 421-438 (2017).

27. Knutson, T. R. et al. Tropical cyclones and climate change assessment: Part II. Projected response to anthropogenic warming. Bull. Am. Meteorol. Soc. 101, E303-E322 (2020).

28. GADM. Database of Global Administrative Areas, version 4.1 (GADM, 2024).

29. Eyring, V. et al. Overview of the Coupled Model Intercomparison Project Phase 6 (CMIP6) experimental design and organization. Geosci. Model Dev. 9, 1937-1958 (2016).

30. O'Neill, B. C. et al. The Scenario Model Intercomparison Project (ScenarioMIP) for CMIP6. Geosci. Model Dev. 9, 3461-3482 (2016).

31. Tatebe, H. et al. Description and basic evaluation of simulated mean state, internal variability, and climate sensitivity in MIROC6. Geosci. Model Dev. 12, 2727-2765 (2019).

32. Swart, N. C. et al. The Canadian Earth System Model version 5 (CanESM5.0.3). Geosci. Model Dev. 12, 4823-4873 (2019).

33. Dunne, J. P. et al. The GFDL Earth System Model version 4.1 (GFDL-ESM 4.1): overall coupled model description and simulation characteristics. J. Adv. Model. Earth Syst. 12, e2019MS002015 (2020).

34. Boucher, O. et al. Presentation and evaluation of the IPSL-CM6A-LR climate model. J. Adv. Model. Earth Syst. 12, e2019MS002010 (2020).

35. Yukimoto, S. et al. The Meteorological Research Institute Earth System Model version 2.0, MRI-ESM2.0: description and basic evaluation of the physical component. J. Meteorol. Soc. Jpn 97, 931-965 (2019).

36. Wu, T. et al. The Beijing Climate Center Climate System Model (BCC-CSM): the main progress from CMIP5 to CMIP6. Geosci. Model Dev. 12, 1573-1600 (2019).

37. Mauritsen, T. et al. Developments in the MPI-M Earth System Model version 1.2 (MPI-ESM1.2) and its response to increasing CO2. J. Adv. Model. Earth Syst. 11, 998-1038 (2019).

38. Volodin, E. M. et al. Simulation of the present-day climate with the climate model INMCM5. Clim. Dyn. 49, 3715-3734 (2017).

39. Zhang, X. et al. Indices for monitoring changes in extremes based on daily temperature and precipitation data. WIREs Clim. Change 2, 851-870 (2011).

40. Van Wagner, C. E. Development and Structure of the Canadian Forest Fire Weather Index System. Forestry Technical Report 35 (Canadian Forestry Service, 1987).

41. Vitolo, C., Di Giuseppe, F., Krzeminski, B. & San-Miguel-Ayanz, J. A 1980-2018 global fire danger re-analysis dataset for the Canadian Fire Weather Indices. Sci. Data 6, 190032 (2019).

42. Di Giuseppe, F., Vitolo, C., Krzeminski, B., Barnard, C., Maciel, P. & San-Miguel, J. Fire Weather Index: the skill provided by the European Centre for Medium-Range Weather Forecasts ensemble prediction system. Nat. Hazards Earth Syst. Sci. 20, 2365-2378 (2020).

43. World Bank. Non-life insurance premium volume to GDP (%) (GFDD.DI.10). Global Financial Development Database (World Bank, 2022).

44. World Bank. Insurance company assets to GDP (%) (GFDD.DI.11). Global Financial Development Database (World Bank, 2022).

45. World Bank. Revenue, excluding grants (% of GDP) (GC.REV.XGRT.GD.ZS). World Development Indicators (World Bank, 2026).

46. World Bank. Central government debt, total (% of GDP) (GC.DOD.TOTL.GD.ZS). World Development Indicators (World Bank, 2026).

47. Notre Dame Global Adaptation Initiative. ND-GAIN Country Index Methodology (ND-GAIN, 2025).

48. Swiss Re Institute 2025 Natural catastrophes: insured losses on trend to USD 145 billion in 2025 sigma 1/2025 (Zurich: Swiss Re Institute)

49. United Nations 2025 Closing the Climate and Disaster Insurance Protection Gap: Thematic Report on Finance (New York: United Nations)

50. World Bank 2026 Disaster Risk Financing and Insurance Program (Washington, DC: World Bank)

51. United Nations Environment Programme 2025 Adaptation Gap Report 2025 (Nairobi: UNEP)

Figures

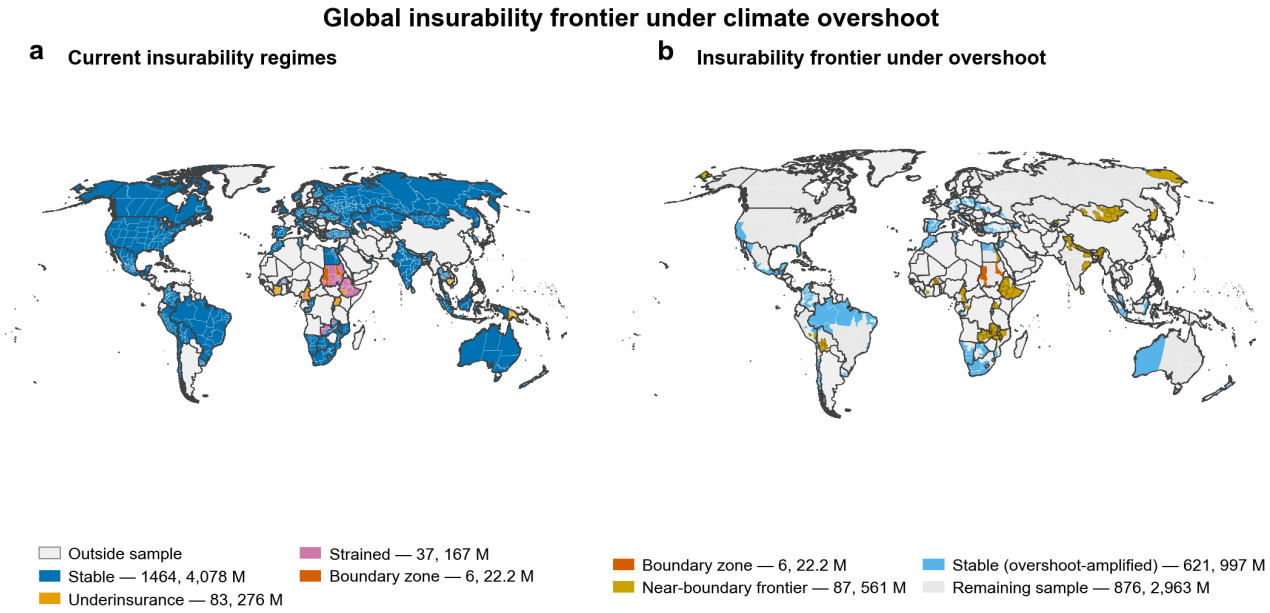

Figure 1 | Global insurability frontier under climate overshoot. a, Current insurability regimes across the final ADM1 sample, classified using overshoot-adjusted climate risk pressure and domestic capacity. b, Insurability frontier under climate overshoot, highlighting the strict boundary zone, the near-boundary frontier and stable regions with overshoot amplification. Grey areas indicate regions outside the analytical sample or sampled regions not highlighted in the frontier classification.

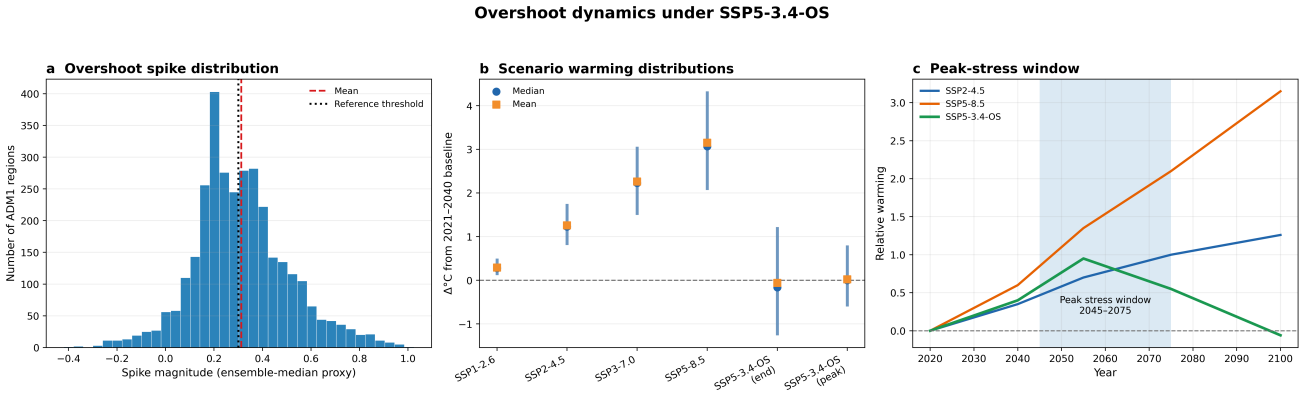

Figure 2 | Overshoot dynamics under SSP5-3.4-OS. a, Distribution of the overshoot spike across ADM1 regions, measured as the ensemble-median difference between mid-century peak warming and end-century warming under SSP5-3.4-OS. b, Scenario warming distributions relative to the 2021-2040 baseline for standard SSP pathways and for the end-century and peak phases of SSP5-3.4-OS. c, Schematic warming trajectories illustrating the mid-century peak-stress window under SSP5-3.4-OS.

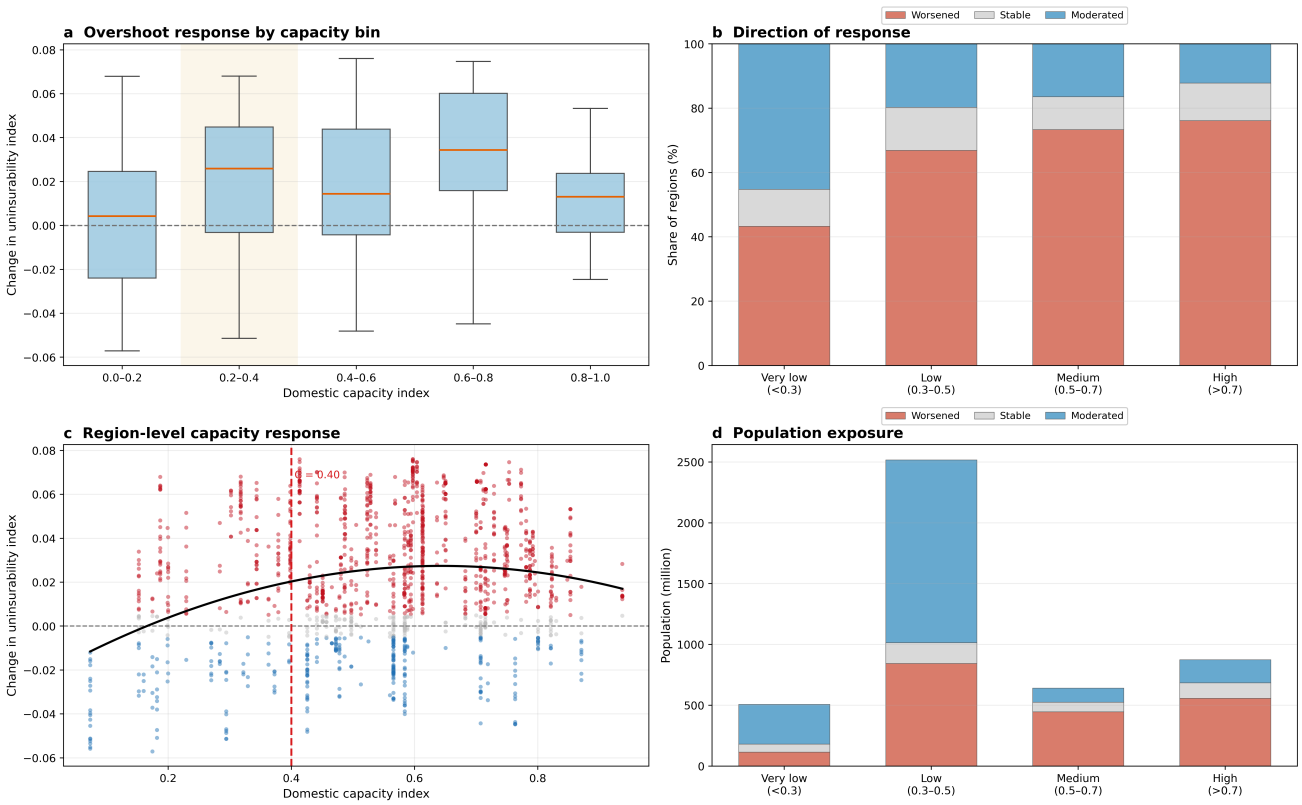

Figure 3 | Domestic capacity and overshoot response. a, Distribution of changes in the uninsurability index across domestic capacity bins. b, Direction of response by capacity tier. c, Region-level relationship between domestic capacity and the change in uninsurability, with the dashed vertical line marking the C = 0.40 reference threshold. d, Population exposure by capacity tier and response direction.

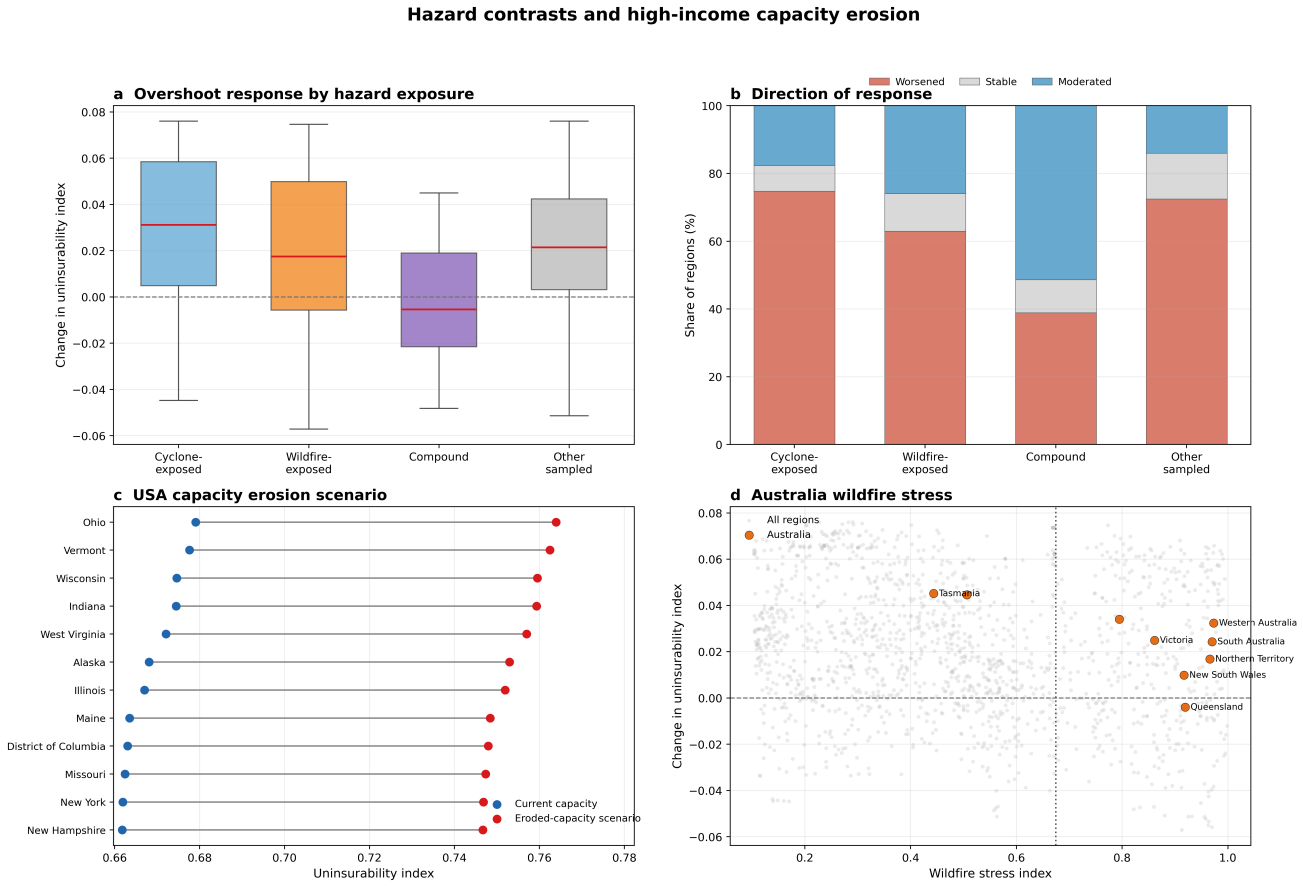

Figure 4 | Hazard contrasts and high-income capacity erosion. a, Distribution of overshoot-related changes in the uninsurability index by dominant hazard exposure. b, Direction of response by hazard class. c, Illustrative USA capacity-erosion scenario showing how reductions in effective domestic capacity can increase uninsurability in high-risk states. d, Australia's wildfire stress profile, showing state-level wildfire exposure against the overshoot-related change in uninsurability.

Tables

Table 1 | Insurability regime distribution under the overshoot-adjusted risk index.

Regime	Regions	Share (%)	Population (M)	Mean UI
Stable insurability	1,464	92.1	4,077.9	0.48
Underinsurance (capacity-limited)	83	5.2	275.8	0.63
Strained insurability	37	2.3	167.3	0.84
Boundary zone (exit risk)	6	0.4	22.2	0.91
Total	1,590	100.0	4,543.3	

Note: Regime classes are assigned at ADM1 level using the interaction between overshoot-adjusted risk pressure (R_pen) and domestic capacity (C). The boundary zone is defined as R_pen > 0.90 and C < 0.20. Population values are reported in millions and may not sum exactly because of rounding.

Table 2 | Boundary-zone regions under the overshoot-adjusted risk framework.

Region	R_pen	R_robust	Capacity	UI	Penalty prob.	FWI	Population (M)
SDN - North Darfur	0.918	0.948	0.073	0.922	0.750	136.1	3.45
SDN - East Darfur	0.903	0.974	0.073	0.912	0.500	107.7	2.13
SDN - West Darfur	0.903	0.996	0.073	0.912	0.375	110.9	0.77
SDN - Kassala	0.902	0.951	0.073	0.912	0.625	113.5	2.42
SDN - River Nile	0.901	0.927	0.073	0.911	0.750	139.1	1.54
BGD - Mymensingh	0.906	0.933	0.199	0.864	0.750	43.7	11.93

Note: Boundary-zone regions jointly exceed the extreme risk-pressure threshold and fall below the very-low-capacity threshold. R_robust denotes the baseline robust climate stress index; R_pen denotes the overshoot-adjusted risk pressure index; UI denotes the overshoot-adjusted uninsurability index. Values are rounded.

Extended Data

Extended Data Table 1 | Near-boundary frontier: highest uninsurability indices outside the boundary zone (top 15 of 87 regions).

Region	ISO3	UI	R_pen	Capacity	Pen. prob.	FWI	WF_SI	Current regime
ETH_Tigray	ETH	0.843	0.859	0.182	0.500	75.5	0.895	Strained
ETH_Beneshangul Gumu	ETH	0.841	0.856	0.182	0.375	72.6	0.881	Strained
BGD_Khulna	BGD	0.838	0.863	0.199	0.625	48.6	0.671	Strained
NPL_Karnali	NPL	0.826	0.958	0.373	0.750	27.5	0.508	Stable
ETH_Somali	ETH	0.822	0.824	0.182	0.625	93.0	0.937	Strained
ETH_Amhara	ETH	0.821	0.823	0.182	0.500	64.2	0.847	Strained
ETH_Gambela	ETH	0.820	0.822	0.182	0.375	63.0	0.834	Strained
BGD_Barisal	BGD	0.820	0.833	0.199	0.750	44.7	0.605	Strained
NPL_Sudurpaschim	NPL	0.818	0.945	0.373	0.750	36.5	0.610	Stable
IND_Ladākh	IND	0.815	0.976	0.426	0.875	20.5	0.350	Stable
ETH_Oromia	ETH	0.811	0.806	0.182	0.500	62.0	0.830	Strained
BOL_Cochabamba	BOL	0.807	0.921	0.363	0.875	29.6	0.265	Stable
ZMB_Eastern	ZMB	0.807	0.858	0.270	0.625	76.7	0.878	Strained
BOL_Oruro	BOL	0.804	0.916	0.363	0.750	96.9	0.563	Stable
CMR_North	CMR	0.804	0.789	0.174	0.250	80.1	0.913	Underinsurance (capacity-limited)

Note: The near-boundary frontier is defined as UI_pen between 0.75 and 0.85 and is not treated as a separate regime. It is included as Extended Data to keep the main display count within the Nature Climate Change limit.